Optical Transition Rates in a Cylindrical Quantum Wire with an Inverse Parabolic Potential

M.Tshipa

Department of Physics, University of Botswana, Private Bag 0022, Gaborone, Botswana,
tshipam@mopipi.ub.bw

ABSTRACT

Transition rates due to electron interaction with circularly polarized radiation in a solid cylindrical nanowire are presented, within the effective mass framework. In particular, the effect of the inverse parabolic potential (superimposed on an infinite cylindrical square well) on transition rates is investigated. As the strength of the potential is swept, transition rates are typified by undulations which stem from the effect of this potential on the wave functions of initial and final states. The potential has the predisposition to reduce transition energies between adjacent states, as such, intensification of the inverse parabolic potential naturally redshifts peaks of transitions rates.

Keywords: Transition rates, confining potentials, cylindrical nanowire

1 INTRODUCTION

Recent advances made in nanotechnology have been rapid, furnishing the scientific community with tools with which to churn out nanostructures of different sizes and geometries [1-3]. These quantum structures can be employed to realize a plethora of devices which utilize different properties of the quantum structures to perform various functions. Some are utilized in biochemical sensing [5, 6], medicine [4, 7], energy generation [8] and optoelectronics [9], among other applications.

The speeds of operation and efficiencies of photonic devices depend on transition rates of the constituent quantum structures; therefore it is imperative to study transition rates in order to better understand how to optimize these devices. Hence, literature is awash with research on transition rates. Xu *et al* studied transition rates for two dimensional quantum cascade lasers [10]. Transition rates were also probed in silicon nanostructures from photoluminescence measurements [11] and in hexagonal shaped nano wires [12].

In this report, electron transition rates due to interaction with circularly polarized radiation in a solid cylindrical nanowire are presented, within the effective mass framework. The confining potential configuration considered here is the inverse parabolic potential superimposed on an infinite cylindrical square well.

2 THEORETICAL FRAMEWORK

2.1 Transition rates

The transition rates from an initial state ψ_i with energy E_i to a final state ψ_f with energy E_f is given by the Fermi Golden rule

$$W_{fi} = \frac{2\pi}{\hbar}\left|\left\langle \psi_f \left| H_{\text{int}} \right| \psi_i \right\rangle\right|^2 \delta\left(E_f - E_i \pm \hbar\omega\right) \qquad (1)$$

where H_{int} describes the electron-photon interaction given by

$$H_{\text{int}} = -\frac{e}{\mu}\vec{A}_\omega \bullet \vec{p} = -\frac{e}{2\mu}A_0\left[e^{i\vec{q}\bullet\vec{r}-\omega t} + c.c\right]\hat{\varepsilon} \bullet \vec{p} \qquad (2)$$

with A_0 being the vector potential amplitude, $\vec{q}$ the photon field wave vector and $\vec{r}$ the electron position vector. c.c is the complex conjugate and $\hat{\varepsilon}$ is the polarization of the radiation. This gives

$$\left\langle \psi_f \left| H_{\text{int}} \right| \psi_i \right\rangle = \frac{eA_0}{2\mu}\left\langle \psi_f \left| e^{i\vec{q}\bullet\vec{r}}\, \hat{\varepsilon} \bullet \vec{p} \right| \psi_i \right\rangle$$

$$\approx \frac{eA_0}{2\mu}\left\langle \psi_f \left| \hat{\varepsilon} \bullet \vec{p} \right| \psi_i \right\rangle$$

$$= \frac{eA_0}{2i\hbar}\left(E_f - E_i\right)\left\langle \psi_f \left| \hat{\varepsilon} \bullet \vec{r} \right| \psi_i \right\rangle \quad (3)$$

The exponential in the second expression has been expanded as a power series $\left(e^{i\vec{q}\bullet\vec{r}} = 1 + i\vec{q}\bullet\vec{r} + \frac{1}{2}(i\vec{q}\bullet\vec{r})^2 + \ldots\right)$, retaining the dominant lowest order terms, while the last expression above has been obtained by utilizing the identity $\vec{p} = \frac{\mu(E_f - E_i)}{i\hbar}\vec{r}$, which springs from the Heisenberg equations of motion for operators. For circularly polarized light $\hat{\varepsilon}\bullet\vec{r} = \rho(\cos\phi \pm \sin\phi)$, where the + (-) is for right (left) circular polarization. Taking the electron wave function as $\psi(\rho, z, \phi) = C_{ml}\chi_{ml}(\rho)e^{ik_z z}e^{im\phi}$, the transition rates are found to be

$$W_{fi}^{abs(em)} = \frac{\pi R^2 e^2 A_0^2 (E_f - E_i)^2}{8\hbar^3 \eta\eta'} |< x >|^2 \times [\delta_{M+1} + \delta_{M-1}]\delta(E_f - E_i \mp \hbar\omega) \quad (4)$$

where $\delta_{M\pm1}$ is the Kronecker delta and $M = m - m'$, with the primes signifying the final state azimuthal quantum number. This implies that the Kronecker delta associated with emission is δ_{M-1} and that associated with absorption is δ_{M+1}. The interaction integral is given by

$$< x >= \int_0^1 x^2 \chi^*_{m'l'}(x)\chi_{ml}\,dx, \text{ while } \eta = \int_0^1 x\chi^2_{ml}(x)\chi_{ml}\,dx$$

and $\eta' = \int_0^1 x\chi^2_{m'l'}(x)\chi_{ml}\,dx$,

where the primes still denote the quantities of the final state. The amplitude of the vector potential A_o can be written as $A_0 = \sqrt{\frac{N_q\hbar}{2\varepsilon_0\varepsilon_m\omega V}}$ where N_q is the number of photons in volume V of the wire of dielectric constant ε_m and ε_0 is the permittivity of free space. Using $\hbar\omega = E_f - E_i$, the absorption transition rate can be expressible as

$$W_{fi}^{abs} = W_0 |< x >|^2 \delta_{M+1}\delta(E_f - E_i - \hbar\omega) \quad (5)$$

and the emmission transition rate as

$$W_{fi}^{em} = W_0 |< x >|^2 \delta_{M-1}\delta(E_f - E_i + \hbar\omega), \quad (6)$$

where $W_0 = \frac{\pi R^2 e^2 A_0^2 (E_f - E_i)^2}{8\hbar^3\eta\eta'}$.

2.2 The wave function

The system considered is one of a cylindrical nanowire of radius R and height L_Z. The nanowire may be a cylindrical *GaAs* material in a host of $Ga_{1-x}Al_xAs$. For this set up, the Schrödinger equation has the form

$$-\frac{\hbar^2}{2\mu}\nabla^2\psi(\rho, z, \phi) + V(\rho)\psi(\rho, z, \phi) = E_T\psi(\rho, z, \phi), \quad (7)$$

where ∇ is the del operator, μ the effective electron mass, $\hbar$ is the reduced Planck's constant and E_T is the total energy of the electron. The electron wave function is sought in the form $\psi(\rho, z, \phi) = C_{ml}\chi(\rho)e^{ik_z z}e^{im\phi}$, where C_{ml} is the normalization constant, k_z is the axial wave number of the electron while m (m = 0, ±1, ±2,...) is the azimuthal quantum number that indicates the angular momentum of an electron. $\chi(\rho)$ is the radial component of the electron wave function which satisfies the Schrödinger equation

$$\frac{1}{\rho}\frac{d}{d\rho}\left(\rho\frac{d}{d\rho}\chi(\rho)\right) - \left\{\frac{2\mu}{\hbar^2}[E_{ml} - V(\rho)] - \frac{|m|^2}{\rho^2}\right\}\chi(\rho) = 0 \quad (8)$$

with E_{ml} being the radial confinement energy of the electron and l is the radial quantum number. The electric potential outside the nanowire is considered to be infinitely high for the electron, while inside the wire has an inverse parabolic potential. The inverse parabolic potential is maximum at the axis of the nanowire and decreases inversely with the square of the radial distance to attain a minimum at the walls (here taken as zero), represented mathematically as

$$V(\rho) = \frac{1}{2}\mu\omega_0^2 R^2\left(\frac{R^2}{\rho^2} - 1\right). \quad (9)$$

After inserting this potential in equation (8), then the solution to the Schrödinger equation is in terms of the Bessel *J* function [13] (the Bessel *Y* being discarded due to its divergent nature at the origin)

$$\chi(\rho) = J_{\nu l}(\kappa\rho), \quad (10)$$

with $\kappa = \sqrt{\frac{\mu\left(2E_{ml} + \mu\omega_o^2 R^2\right)}{\hbar^2}}$ and $v = \sqrt{|m|^2 + \mu^2\omega_o^2 R^4 / \hbar^2}$.

Applying the boundary conditions at the wall of the cylinder ($\rho = R$) avails the electron energy spectrum as

$$E = E_{ml} + \frac{\hbar^2 k_z^2}{2\mu} = \frac{\hbar^2 j_{oml}^2}{2\mu\mu^2} - \frac{1}{2}\mu\omega_o^2 R^2 + \frac{\hbar^2 k_z^2}{2\mu}, \quad (11)$$

where j_{oml} are the zeroes of the Bessel *J* function.

3 RESULTS AND DISCUSSIONS

The value of the electron effective mass used in these computations is $\mu = 0.067 m_e$, where m_e is the electron free mass, pertaining to *GaAs* crystals.

The radial position expectation values of the lower *m* valued states are closer to the wire axis (where the potential is higher) than those of higher states, resulting in the lower *m* valued states being the most susceptible to the inverse parabolic potential. As such, as this potential increases the eigen energies of lower *m* valued states more than those of the higher *m* valued states as it intensifies. This imbues the inverse parabolic potential with the proclivity to dwindle transition energies between adjacent states as it gets stronger. Consequently, intensification of the inverse parabolic potential naturally redshifts peaks of transitions rates, regardless of the value of the radial quantum number *l* (Fig. 1).

The nature of the inverse parabolic potential is such that it 'expels' electrons away from the axis of the wire, towards the walls. This is signified by the shifting of peaks of electron wave functions away from the wire axis. This shifting is accompanied by modulation in amplitudes of the radial component of the wave function at different antinodes. These modulations percolate through to the interaction integral, which is characterized by undulations as the potential strength is swept [13]. The transition rates are not immune to this permeation of undulations which are evident in Figs. 2-4. As the radial quantum number increases, the undulations also increase in number.

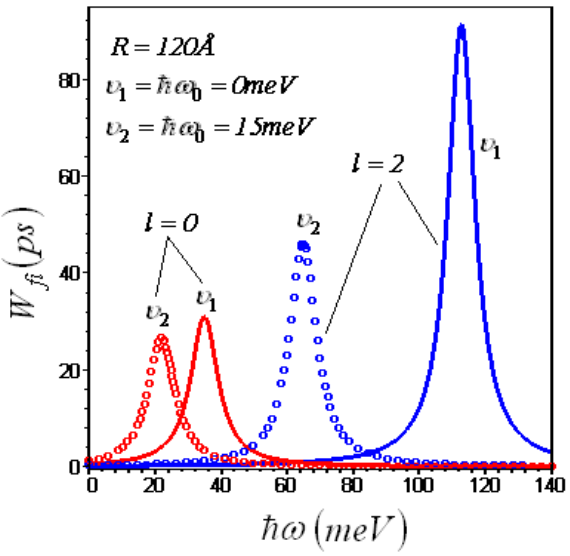

Figure 1: Transition rates as functions of the photon energy for a transition from the ground state to the first excited state. The solid plots are for $\hbar\omega_0 = 0meV$ while the circles are for $\hbar\omega_0 = 5meV$.

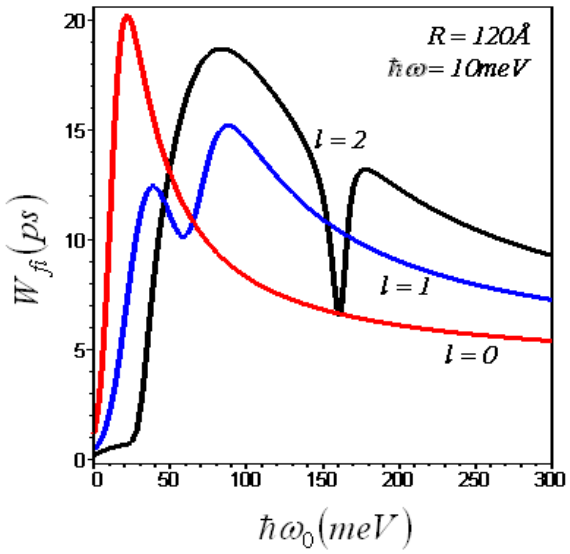

Figure 2: The variation of transition rates (from ground state to first excited state) with strength of the inverse parabolic potential for radial quantum number *l* = 0, 1, and 2.

TechConnect Briefs 2016, TechConnect.org, ISBN 978-0-9975-1173-4

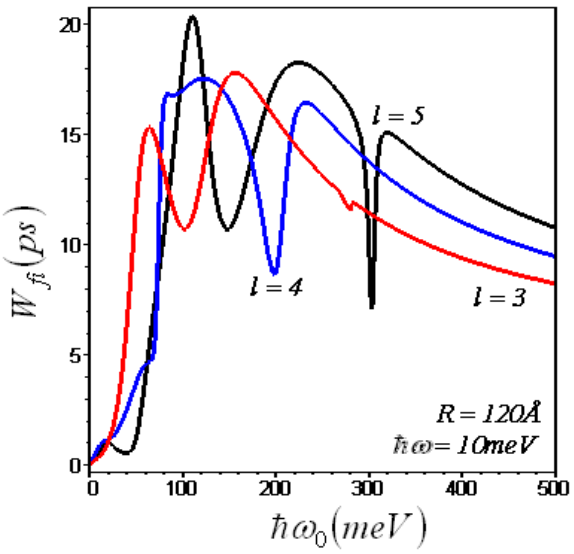

Figure 3: Variation of transition rates as functions of strength of the inverse parabolic potential for the $m=0\rightarrow m=\pm1$ transition for the indicated radial quantum number *l* values.

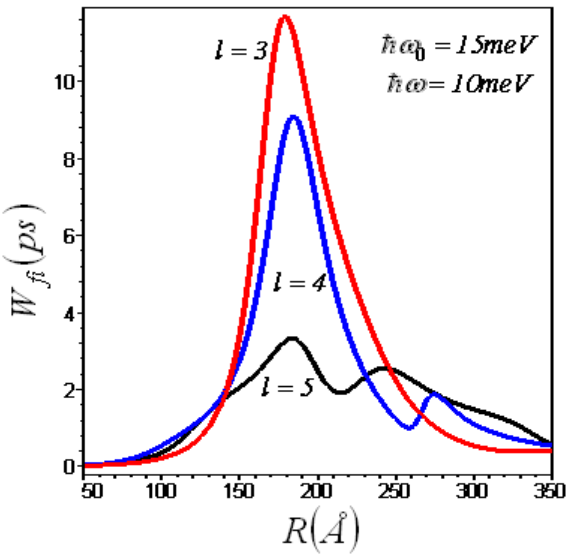

Figure 4: The dependence of the rates of transition on the radius of the quantum wire for given beam energy. The transition is from the ground state to the first excited state.

Transition energies scale inversely with the radius of the nanowire. Thus, increasing the radius redshifts peaks of the transition rates. Correspondingly, as the beam energy is increased, the radii of resonance shift to smaller value. Moreover, transition rates corresponding to small radii (corresponding to higher energy of excitation) are weightier than those corresponding to larger nanowires. For an infinite cylindrical square well ($\hbar\omega_0=0meV$), in order to alter the transition energies in the absence of the magnetic field, one has to vary the radius of the wire; reducing the radius of the wire increases the transition energies, and vice versa. In essence, the nature of the potential offers nanotechnology an opportunity to vary beam energy of excitation without necessarily having to alter the radii of the nanowire, in cases where the dimensions are to have specific values.

4 CONCLUSIONS

The dependence of transition rates on the strength of the inverse parabolic potential has been studied. The transition rates a typified by undulations which increase as the radial quantum number increases. The nature of the potential is such that it decreases the energy gap between adjacent states, thus increase in the strength of this potential redshifts peaks of transition rates. This offers another avenue of tuning nanowires apart from varying the size of the nanostructures.

5 REFERENCES

[1] R. Gunawidjaja, H. Diez-y-Riega and H. Eilers, "Synthesis and characterizations of spherical Eu:La_2O_3 and related core/shell nanoparticles", Powder Technol 271, 255, (2015).

[2] K. Anandan and V. Rajendran, "Sheet, spherical and plate-like chromium sesquioxide (Cr_2O_3) nanostructures synthesized via ionic surfactants assisted facile precipitation method", Mater. Lett. 146, 99, 2015.

[3] I. Kontopoulou, A. Angelopoulou and N. Bouropoulos, "ZnO spherical porous nanostructures onbtained by thermal decomposition of zinc palmitate", Mater. Lett. 165, 87, 2016.

[4] D. Irawan, T. Saktioto, J. Ali and P. Yupapin, "Design of Mach-Zehnder interferometer and ring resonator for biochemical sensing", Photonic Sensors 5, 12, 2015.

[5] Y. Shi, H. Guo, J. Yang, M. Zhao, J. Liu, C. Xue and J. Tang, "Plasma-induced wafer-scale self-assembly of silver nanoparticles and application to biochemical sensing", Materials 8, 3806, 2015.

[6] G. G. Walmsley, A. McArdle, R. Tevlin, A. Momeni, D. Atashroo, M. S. Hu, A. H. Feroze, V. W. Wong, P. H. Lorenz, M. T. Longaker and D. C. Wan, "Nanotechnology in bone tissue

engineering", Nanomed-Nanotechnol 11, 1253, 2015.
[7] F. Shi, Y. Zhang, C. Yang, T. Guo and N. Feng, "Preparation of a micro/nanotechnology based multi-unit drug delivery system for a Chinese medicine Niuhuang Xingxiao Wan and assessment of its antitumor efficacy", Int. J. Pharm. 492, 244, 2015.
[8] L. Mo, L. Yang, E. H. Lee, S. He, "High-efficiency plasmonic metamaterial selective emitter based on an optimized spherical core-shell nanostructure for planar solar thermovoltaics", Plasmonics 10, 529, 2015.
[9] F. Najafi, A. Dane, F. Bellei, Q. Zhao, K. A. Sunter, A. N. McCaughan and K. K. Berggren, "Fabrication process yielding saturated nanowire single-photon detector with 24-ps jitter", IEEE J. Sel. Top. Quant. 21, 3800507, 2015.
[10] J. Xu, L. Liu, B. H. Li, Z. Zhang, J. Ma, K. Liu, J. He and D. Z. Shen, "Quantum cascade lasers designed toward shorter wavelengths", J. Phys.: Condens. Matter 25, 065302, 2016.
[11] F. Sangghaleh, I. Sychugov, Z. Yang, J. G. C. Veinot and J. Linnros, "Near-unity internal quantum efficiency of luminescent silicon nanocrystals with ligand passivation", ACS Nano 9, 7097, 2015.
[12] V. U. Chimalgi, Md. R. K. Nishat and S. S. Ahmed, "Nonlinear polarization and efficiency *droop* in hexagonal InGaN/GaN disk-in-wire LEDs", Superlattice. Microst. 84, 91, 2015.
[13] M. Tshipa, "Oscillator strength for optical transitions in a cylindrical quantum wire with an inverse parabolic confining electric potential", Indian J. Phys. 88, 849, 2014.